

# A non-Boussinesq integral method for laminar free convection between vertical flat plates subject to a uniform wall heat flux

M. A. LANGERMAN

South Dakota School of Mines & Technology, Rapid City, SD 57701-3995, U.S.A.

(Received 20 July 1992 and in final form 17 February 1993)

**Abstract**—An integral method is developed to analyze laminar free convection between large aspect ratio, vertical, parallel plate channels subject to a uniform, symmetric, heat flux and varying fluid properties. The flow is assumed to be fully developed, which is a good assumption for channels with large aspect ratios. This is a heat transfer problem characterized by high temperature ratios, thereby rendering the commonly applied Boussinesq approximation invalid. The method developed is general and, therefore, can be used to calculate natural circulation of gases or liquids. Sample calculations are included for air between 300 and 1100 K.

## INTRODUCTION

NATURAL convection flows occur in many areas of applied engineering including nuclear reactor cooling systems, atmospheric and oceanic circulation and electric machinery. The flow is a buoyancy-induced motion resulting from body forces acting on density gradients which, in turn, arise from temperature and/or mass concentration gradients in the fluid.

The problem of cooling heated, vertical, parallel plates by natural convection has drawn considerable attention, primarily due to the interest generated within the electronics industry. The history of the modeling of such problems has been a sequence of refinements and successive approximations [1]. Elenbaas [2], in early measurements, showed that the Nusselt number,  $Nu$ , is proportional to the channel Rayleigh number,  $Ra$ . Aung [3] studied the problem of symmetric and asymmetric heating of the plates and presented results indicating that the thermal development length is independent of the Prandtl number,  $Pr$ . This was a surprising result due to its distinction from that of forced convection, where it is well known that the ratio of the development length for velocity and temperature is a function of  $Pr$ . Ramanathan and Kumar [1] showed later, however, that Aung's result is valid only in the range of aspect ratios where axial diffusion (not accounted for in Aung's model) is no longer significant ( $L/b \geq 15$ ). At these relatively high aspect ratios and corresponding low  $Ra$  ( $Ra \leq 0.14$ ), Aung *et al.* [4], as reported in ref. [1], found that the flow may be considered fully developed along most of the channel. The experiments of Wirtz and Stutzman [5] agree well with the analytical model of Aung.

The efforts to model natural circulation cited above were developed for processes involving small temperature differences or low temperature ratios,  $T_R$ , where  $T_R$  is defined as the ratio of the channel outlet

mean fluid temperature to the channel average fluid temperature. With a low  $T_R$ , the process is amenable to the simplifying Boussinesq approximation, which is commonly understood [6] to consist of the assumptions that (a) the fluid properties are constant except density in the momentum equation when it directly causes buoyant forces, and (b) viscous dissipation is negligible. There exists a class of problems, however, where heat transfer rates are high enough to render the first of these assumptions invalid. These problems are characterized by a high  $T_R$ , for example, heat transfer along nuclear fuel plates of test reactors [7]. Although the effects of variable properties have been studied for different geometries (see refs. [8, 9]), no methods were found for resolving this non-Boussinesq problem for vertical channel geometries. Therefore, an analytical investigation was conducted to study this variable fluid property heat transfer problem. The results obtained are the subject of this paper.

## PROBLEM STATEMENT

The approach is to model the system using the integral boundary layer equations. The flow is assumed to be fully developed, laminar flow. Aung *et al.* [4] showed that neglecting the thermal and hydrodynamic entry lengths produced reasonable results for  $Ra < 100$ . Miyamoto *et al.* [10] showed that characterizing the flow as laminar flow is valid for  $Pr Gr_L \leq 10^{10-11}$ . These limits are implied in this application.

Since the velocity along the channel will vary inversely with the density as heat is added, the characterization of fully developed flow is, therefore, conveyed in the same sense as a fully-developed temperature profile in the case of constant fluid properties. That is, only the ratio of the local velocity to



The facility in applying the integral boundary layer approach lies in the resulting solution of ordinary differential equations as opposed to partial differential equations (for a discussion see ref. [12]). This approach, however, requires representations for the velocity and temperature distributions and the wall shear stress. Indeed, the solution accuracy is dependent upon these representations. Langerman and Bayless [7] showed that, for laminar, Newtonian flow, simple parabolic distributions produced results, for low  $Ra$ , indistinguishable from those of Aung [3]. These distributions are used in this analysis and are given here in terms of the mean channel velocity,  $V$ , the mean channel outlet temperature,  $T_m$ , and channel outlet surface temperature,  $T_0$ , as

$$u = \frac{3}{2}V\eta(2-\eta), \quad (4)$$

and

$$T = T_0 + \frac{5}{4}(T_0 - T_m)\eta(\eta - 2), \quad (5)$$

where  $\eta = y/l$ .

Here, as in most natural circulation analyses, the density is cast as a linear function of temperature. In doing so, compressibility effects are neglected, which is a good approximation for thermally induced natural convection problems (see refs. [6, 13]). Using a Taylor series expansion around some reference value of  $T$ , say  $\bar{T}$ , and neglecting higher-order terms, results in

$$\rho = \bar{\rho}[1 - \beta(T - \bar{T})], \quad (6)$$

where  $\beta$  is the coefficient of thermal expansion defined as

$$\beta = -\frac{1}{\bar{\rho}} \left( \frac{\partial \rho}{\partial T} \right)_p \quad (7)$$

For fluids which approximate ideal gases over a limited temperature range (e.g. air between 300 and 1100 K),  $\beta = 1/\bar{T}$ .

#### *Boussinesq model*

If  $\bar{T}$  in equation (6) is defined as the average channel fluid temperature,  $\bar{T}$ , and assuming the pressure gradient is due solely to the weight of the fluid, then equation (2) reduces to [7]

$$V = \left( \frac{l^2}{3\bar{\mu}} \right) \bar{\rho} \bar{\beta} g [(T_0 - \bar{T}) - \frac{5}{4}(T_0 - T_m)], \quad (8)$$

where the tilde signifies average values over the entire channel length. Note, the assumption regarding the pressure gradient is true, in the strictest sense, only under hydrostatic conditions, but is approached closely at low velocities and for  $\Delta\rho/\bar{\rho} \ll 1$ , or equivalently  $\bar{\beta}(T - \bar{T}) \ll 1$ , along the channel. This latter stipulation, if met, renders the Boussinesq approximation valid for the case of air flow (see Gebhart [13]).

*Remark.* In their work, Gray and Giorgini [6] indicate that  $\bar{\beta}(T - \bar{T}) \leq 10^{-1}$  (with the same constraint

on the remaining fluid properties) is sufficient for Boussinesq flow. Langerman and Bayless [7] relaxed this criteria to  $\bar{\beta}(T - \bar{T}) \leq 0.25$  in their study of air flow.

Equations (4) and (5) are substituted into equation (3) to provide a relationship for the channel outlet fluid temperature,  $T_m$ . Fourier's law is used to relate the surface temperature,  $T_0$ , to the fluid temperature,  $T_m$ , at the channel outlet. This temperature information is substituted into equation (8) and, after rearranging, results in

$$V = \left( \frac{l^2}{3\bar{\mu}} \right) \bar{\rho} \bar{\beta} g \left( q'' \frac{b}{k} \right) (\bar{\theta} - \frac{1}{5}), \quad (9)$$

where  $\bar{\theta}$  is the non-dimensional temperature defined as  $\bar{\theta} = (T_0 - \bar{T})/[q''(b/k)]$ . It is easily shown, from a simple energy balance, that  $\bar{\theta}$  is related to the non-dimensional channel velocity,  $V^*$ , as

$$\bar{\theta} = \frac{1}{V^*} + \frac{1}{5}, \quad (10)$$

where

$$V^* = \frac{Pr V b^2}{\bar{\nu} L}. \quad (11)$$

With equation (11) substituted, equation (9) reduces to

$$V^* = \left( \frac{1}{12} \right) Ra \left( \frac{1}{V^*} + \frac{1}{30} \right). \quad (12)$$

For  $Ra < 100$ , the constant  $1/30$  in equation (12) can be neglected and

$$V^* \approx 0.2887 \sqrt{(Ra)}, \quad (13)$$

which is identical to the result reached by Aung [3] using the partial differential equations of the boundary layer.

It is easily verified that, under low flow and heat transfer rates, the Boussinesq approximation is a good approximation. Langerman and Bayless [7] showed that the above Boussinesq model produced results that are in agreement with those of Aung for  $Ra < 100$ . They went on to show, however, that when heat transfer rates are high or channel aspect ratios are large, the Boussinesq approximation may break down. The following section presents a method for calculating the heat transfer for problems where the Boussinesq model has questionable applicability.

#### *Non-Boussinesq (variable properties) model*

With relatively high heat fluxes, the temperature rise along the channel length may become significant and the assumption regarding constant properties must be reevaluated. Returning to equation (2) with the density relationship defined by equation (6) but including the pressure and fluid weight terms results in

$$-\frac{d}{dx} \int \rho u^2 dy - \tau_0 + \tilde{\rho} g \tilde{\beta} \int (T - \tilde{T}) dy - \frac{d\tilde{p}}{dx} l - \tilde{\rho} g l = 0, \quad (14)$$

where  $d\tilde{p}/dx$  is an estimate of the pressure gradient which, as discussed later, is obtained elsewhere. From equation (14), and a relationship for viscosity analogous to that for density, equation (6), an equation similar to equation (8) is obtained as

$$\frac{dV}{dx} = -\frac{2.5\tilde{\mu}[1 + \tilde{\sigma}(T_0 - \tilde{T})]}{\tilde{\rho} l^2 [1 + 2\tilde{\beta}(\tilde{T} - T_m)]} + \frac{g\tilde{\beta}}{V[1 + 2\tilde{\beta}(\tilde{T} - T_m)]} [\frac{5}{6}(T_0 - \tilde{T}) - \frac{5}{36}(T_0 - T_m)] - \frac{5}{6V[1 + 2\tilde{\beta}(\tilde{T} - T_m)]} \left( \frac{1}{\tilde{\rho}} \frac{d\tilde{p}}{dx} + g \right), \quad (15)$$

where  $\tilde{\sigma}(T_0 - \tilde{T})$  accounts for the change in viscosity around  $\tilde{T}$  and essentially admits another 'body force' like term to the equation of motion. Equation (15) is an ordinary differential equation in  $V$ . This 'initial-value' type problem is particularly well suited to higher-order solution techniques such as Runge-Kutta, provided some estimate of the pressure gradient can be obtained. For convenience, equation (15) is cast in non-dimensional form by introducing a non-dimensional pressure,  $\hat{p}^*$ , and distance,  $x^*$ , as

$$\hat{p}^* = \frac{(\hat{p} - p_0)h^3}{\tilde{\rho}\tilde{\nu}^3 GrL}, \quad x^* = \frac{x}{L}, \quad (16)$$

where  $p_0$  is the hydrostatic pressure at  $x$ . Equation (15) then reduces to

$$\frac{dV^*}{dx^*} = \frac{\tilde{Pr}\tilde{Ra}}{V^*\tilde{\omega}} \left[ \frac{5}{6} \left( \frac{\Delta x^*}{V^*} - \frac{d\hat{p}^*}{dx^*} \right) + \left( \frac{1}{36} \right) \right] - 10\tilde{Pr} \left( \frac{\tilde{\psi}}{\tilde{\omega}} \right), \quad (17)$$

where  $\tilde{\psi} = 1 + \tilde{\sigma}(T_0 - \tilde{T})$ , and  $\tilde{\omega} = 1 + 2\tilde{\beta}(\tilde{T} - T_m)$ . In practice,  $\tilde{\psi}, \tilde{\omega} \rightarrow 1$  as  $\Delta x^* \rightarrow 0$ . The problem described by equation (17) is not particularly amenable to dimensional analysis since  $\tilde{Ra}$  and, to a lesser extent,  $\tilde{Pr}$  are local parameters that vary along the channel. Note that the tildes in equations (15) and (17) now represent average values along an incremental channel length. Also note that, for Boussinesq conditions (i.e.  $dV^*/dx^* = d\hat{p}^*/dx^* = 0$  and  $\tilde{\psi} = \tilde{\omega} = \Delta x^* = 1$ ), equation (17) reduces to equation (12) as expected.

The solution begins by specifying a channel wall heat flux and mass flow rate. The local values of  $\tilde{Pr}$  and  $\tilde{Ra}$  are determined and equation (17) is integrated along an incremental length of the channel as opposed to the Boussinesq model, equation (12), which was obtained by integrating along the entire length of the channel in one step. The estimated pressure gradient is then modified, if necessary, until the resulting mass flow rate at the outlet of the incremental channel distance equals that at the inlet, thus satisfying con-

tinuity, equation (1). This procedure is continued along the entire channel length at which point the outlet pressure,  $\hat{p}^*$ , is compared to the implied null boundary condition,  $\hat{p}^* = 0$ . If a significant difference results, the calculation is restarted with a newly assumed value of the mass flow rate and the loop continued until  $\hat{p}^* \leq \epsilon$ , where  $\epsilon$  is an acceptable numerical measure of zero.

The pressure convergence rate is strongly influenced by the initial estimate of the pressure gradient as well as the algorithm for modifying the pressure gradient during the iteration process. Discussed below is a method used to estimate the initial value of the pressure gradient term, which, when coupled with the subsequent updating algorithm, produces a rapid rate of convergence.

#### Pressure-velocity coupling

The method is a variation of the one introduced by Patankar and Spalding [14], and later used by Baker [15], but with buoyancy terms included. The approach is basically an integral approach representing the initial estimate of the pressure gradient as

$$\left. \frac{d\hat{p}^*}{dx^*} \right|_{\text{initial}} = \left[ -\frac{12V^*}{\tilde{Ra}} - \frac{V^{*2}\tilde{\beta}}{\tilde{Pr}\tilde{Ra}} \left( \frac{1}{\Delta x^*} \right) + \tilde{\omega} - \frac{1}{6} \right]. \quad (18)$$

All the information on the right hand side of equation (18) is available, thus providing a means for obtaining a first estimate of the pressure gradient. This estimate is then updated using

$$\left. \frac{d\hat{p}^*}{dx^*} \right|_{\text{next}} = \left. \frac{d\hat{p}^*}{dx^*} \right|_{\text{last}} + \Delta \left( \frac{d\hat{p}^*}{dx^*} \right), \quad (19)$$

where the  $\Delta(\ )$  correction term will drive the solution towards a numerical measure of continuity. From the continuity equation and a simplified form of the one-dimensional momentum equation, it can be shown that the correction term takes the form [16],

$$\Delta \left( \frac{d\hat{p}^*}{dx^*} \right) = - \left[ \frac{2V^*(\Delta V^*)}{\Delta x^*} \right] \left( \frac{\tilde{R}}{\tilde{Pr}\tilde{Ra}} \right), \quad (20)$$

where  $\Delta V^*$  is the difference between  $V^*$  obtained with the known mass flow rate and fluid state changes over  $\Delta x^*$  and  $V^*$  obtained from equation (17).

#### NUMERICAL ACCURACY

The accuracy of the present method has been assessed numerically through successive grid reductions and conceptually through comparisons with model results from Aung *et al.* [4], and with experimental data from Wirtz and Stutzman [5]. This latter, conceptual assessment, was made at conditions for which the assumption of constant fluid properties is warranted. Outside the limits of Boussinesq flow, no data or model results were found for comparison,

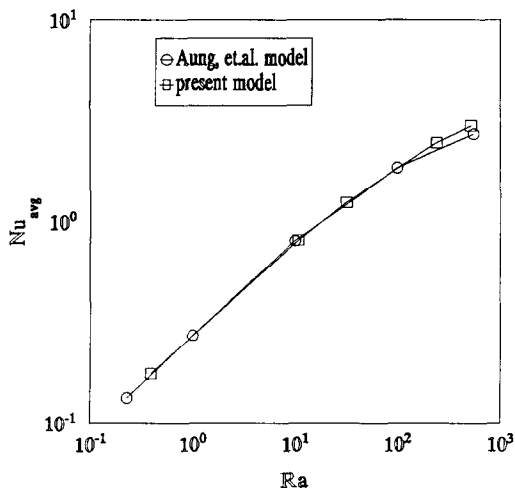


FIG. 2. Average channel Nusselt number.

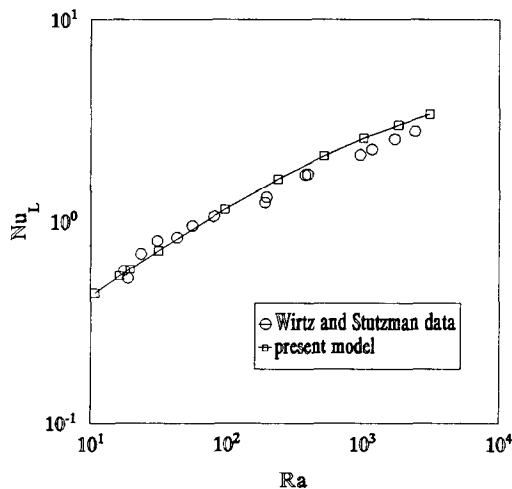


FIG. 3. Channel outlet Nusselt number.

although the results obtained here seem reasonable from an engineering judgment point of view.

A fourth order Runge–Kutta numerical scheme was used to solve equation (17). A successive axial grid refinement exercise led to the choice of 100 equally spaced axial steps. At higher grid refinements, little difference in calculated results was realized, however, on occasion it was necessary to reduce the space step even further to enhance pressure–velocity convergence. The minimum  $\Delta x^*$  required in the calculations performed was  $10^{-3}$ .

Figure 2 compares the present model results to those from Aung *et al.* [3]. The comparison shown is for the Nusselt number,  $Nu$ , where  $Nu$  is defined as

$$Nu = \frac{q''b}{(T_0 - T_x)k} \tag{21}$$

In Fig. 2, the average channel Nusselt number,  $Nu_{avg}$ , is presented, consequently  $T_0$  in equation (21) was evaluated at the channel mid height. For  $Ra < 100$ , the results from the present model are indistinguishable from those of Aung. For  $Ra > 100$ , hydrodynamic entry length effects begin to become important and the results from the present model start to deviate from those of Aung.

Figure 3 compares the channel outlet Nusselt number,  $Nu_L$ , calculated with the present model compared with experimental data (Wirtz and Stutzman [5]). Again, the analytical results are in good agreement with the data for  $Ra < 100$  and tend to over predict the data at larger  $Ra$ .

**NUMERICAL RESULTS**

The fluid considered here is air for  $300 \leq T \leq 1100$  K. The channel aspect ratio,  $R$ , was varied from 50 to 500. The applied heat flux was varied over an order of magnitude from 10–150  $W m^{-2}$ .

Figure 4 compares  $Nu_L$  obtained from the Boussinesq model and the non-Boussinesq model. As indicated,

as  $Ra$  decreases, the Boussinesq model soon becomes invalid even at relatively low values of channel heat flux. Also the results obtained from the non-Boussinesq model do not correlate to a single curve but are a function of the applied heat flux with a higher flux causing, as expected, an earlier departure from the Boussinesq curve (as  $Ra$  is decreased). Conversely, the non-Boussinesq results approach the Boussinesq curve asymptotically with increasing  $Ra$ .

Langerman and Bayless [7] argued that, for air flow conditions and  $T_R > 1.25$ , the Boussinesq model will under predict the channel heat transfer rate. This conclusion was based upon examination of the product  $\beta(T - \tilde{T})$  as the channel heat flux was increased. Recall that, for Boussinesq flow conditions,  $\beta(T - \tilde{T}) \ll 1$ . They chose to assign as the limit for this product a value of 0.25, which was exceeded for  $T_R > 1.25$ . As

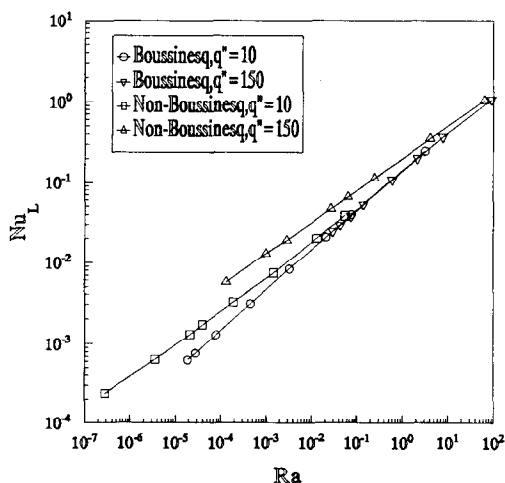


FIG. 4. Channel outlet Nusselt number, Boussinesq and non-Boussinesq models.

will be shown, results presented here are in agreement with their result.

The ratio of non-Boussinesq to Boussinesq output was found to be a convenient format for assessing the calculated results. It was determined that these ratios correlate to a group of non-dimensional parameters evaluated at ambient conditions and using a characteristic dimension equal to the overall channel length. Specifying this group as  $\Lambda$ , then

$$\Lambda = \sqrt{\left(\frac{Gr_L Fr_L^2}{Re_L^2} \left(\frac{R^3}{S^3}\right)\right)}, \quad (22)$$

where  $S$  is the ratio of channel length to unit depth. It is not surprising that  $Gr$ ,  $Fr$ , and  $Re$  occur in equation (22) since these numbers result directly from a non-dimensional analysis of the Navier-Stokes equations. It can be shown that this group of three non-dimensional numbers is equivalent to a non-dimensional heat flux,  $\Phi$ , defined as

$$\Phi = \frac{q''L}{(Tk)_x}. \quad (23)$$

Hence,

$$\Lambda = \sqrt{\left(\Phi \left(\frac{R^3}{S^3}\right)\right)}. \quad (24)$$

Equation (24) provides a more intuitive approach to evaluating the calculated results.

For example, Fig. 5 shows the ratio of the mass flow rates vs  $\Lambda$  obtained at  $q'' = 10$ , and  $150 \text{ W m}^{-2}$ . At  $\Lambda \approx 7.5 \times 10^3$ , the non-Boussinesq model begins to calculate a higher flow rate and by  $\Lambda \approx 10^4$ , the flow rate calculated with non-Boussinesq model is approximately 20% higher than that calculated with the Boussinesq model. Similarly, the ratio of the outlet Nusselt numbers shown in Fig. 6 begins to reflect a higher heat transfer rate obtained with the non-

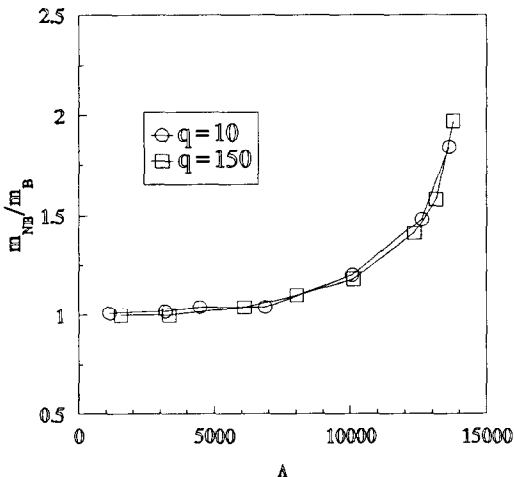


FIG. 5. Ratio of the calculated mass flow rates,  $T_x = 300 \text{ K}$ .

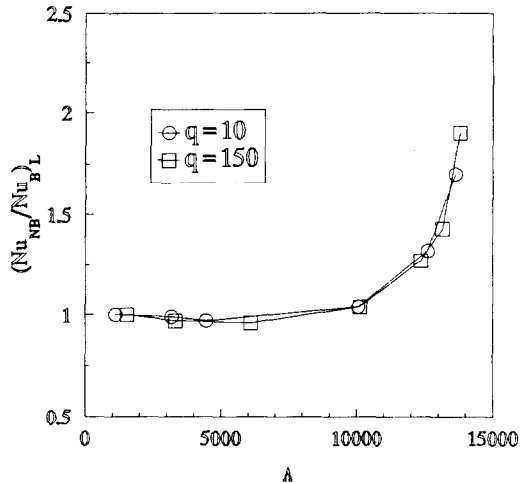


FIG. 6. Ratio of the calculated Nusselt numbers,  $T_x = 300 \text{ K}$ .

Boussinesq model for  $\Lambda > 7.5 \times 10^3$ , but the difference is not significant until  $\Lambda \geq 10^4$ . As indicated in Fig. 7, at  $\Lambda = 10^4$  the temperature ratio,  $T_R$  is approximately 1.25 which agrees with the result of Langerman and Bayless [7] cited earlier.

The results shown in Figs. 5-7 indicate that, for  $\Lambda \geq 10^4$ , the Boussinesq model will under predict the channel heat flux. Figure 8 presents a plot of equation (24) for  $\Lambda = 10^4$  and, given a channel aspect ratio,  $R/S$ , indicates the limiting value of  $\Phi$  for which the Boussinesq model is appropriate.

The curves presented in Figs. 5-8 may be used to calculate specific heat transfer results for air flow problems that fall within the limits of the data presented. For example, to determine  $Nu_L$  given  $R = 215$ ,  $S = 1$ ,  $q'' = 150 \text{ W m}^{-2}$  and  $T_x = 300 \text{ K}$  ( $k = 0.026 \text{ W m}^{-1} \text{ K}^{-1}$ ), first calculate  $\Lambda$  from equations (23) and (24) as

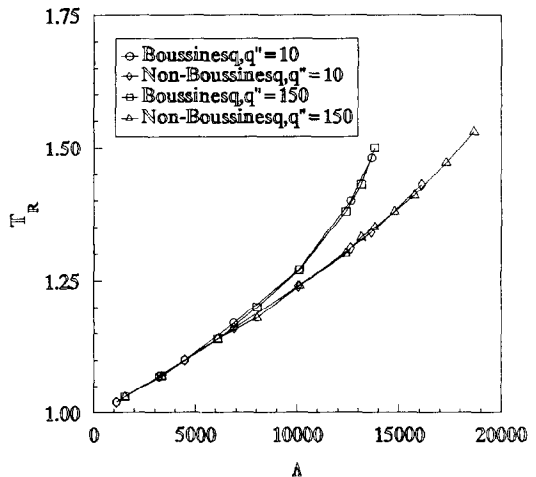


FIG. 7. Temperature ratio,  $T_x = 300 \text{ K}$ .

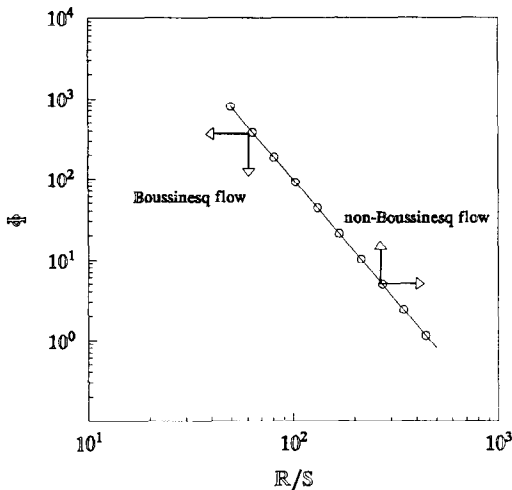


FIG. 8. Non-dimensional heat flux vs aspect ratio.

$$\Lambda = \sqrt{\left(\frac{150(1)}{300(0.026)}(215)^3\right)} \approx 1.40 \times 10^4 > 10^4.$$

$T_R$  from Fig. 7 is estimated to be

$$T_R \approx 1.35$$

from which

$$T_{m,L} = \frac{T_R T_\infty}{2 - T_R} = 623 \text{ K}.$$

At 623 K,  $k \approx 0.045 \text{ W m}^{-1} \text{ K}^{-1}$ , then from Fourier's law and equation (5),

$$T_{0,L} - T_{m,L} = q''(b/k)/5 \approx 3 \text{ K}$$

so

$$T_{0,L} \approx 626 \text{ K}.$$

$Nu_{NB}$  from equation (21) and  $T_{0,L} = 626 \text{ K}$  is

$$Nu_{NB} = \frac{150(1/215)}{326(0.045)} = 4.76 \times 10^{-3},$$

which is within 2% of  $4.66 \times 10^{-3}$ , the  $Nu_{NB}$  calculated with the model described in the previous sections.

Similarly, if  $q''$  is sought given  $T_{0,L}$ ,  $T_\infty$ ,  $R$  and  $S$ , then the procedure is the same, however, in this case,  $q''$  is assumed and the resulting  $T_{0,L}$  is compared with the known value. If a significant difference exists, the assumed value of  $q''$  is modified and the procedure repeated.

## CONCLUSIONS

A non-Boussinesq integral method for laminar free convection between vertical flat plates subject to a uniform, symmetric wall heat flux has been developed in this study. Numerical solutions to the two-dimensional integral boundary layer equations have been obtained, and, as  $Ra$  increases, have been shown to asymptotically approach the closed form solution for fully developed Boussinesq flow. It has been shown

that for air flow, a  $\Lambda > 10^4$  results in non-Boussinesq flow conditions, where  $\Lambda$  is a non-dimensional parametric combination of the applied wall heat flux and the channel aspect ratio.

*Acknowledgements*—This work was supported by the U.S. Department of Energy Assistant Secretary for Office of Nuclear Energy, under DOE Contract No. DE-AC07-761D01570 and the INEL Long Term Research Initiative in Computational Mechanics.

## REFERENCES

1. S. Ramanathan and R. Kumar, Correlations for natural convection between vertical plates heated asymmetrically, *J. Heat Transfer* **113**, 97–107 (1991).
2. W. Elenbaas, Heat dissipation of parallel plates by free convection, *Physica* **9**, 1–28 (1942).
3. W. Aung, Fully developed laminar free convection between vertical plates heated asymmetrically, *Int. J. Heat Mass Transfer* **15**, 1577–1580 (1972).
4. W. Aung, L. S. Fletcher and V. Sernas, Developing laminar free convection between vertical plates with asymmetric heating, *Int. J. Heat Mass Transfer* **16**, 2293–2308 (1972).
5. T. A. Wirtz and R. J. Stutzman, Experiments on free convection between vertical plates with symmetric heating, *J. Heat Transfer* **104**, 501–507 (1982).
6. D. D. Gray and A. Giorgini, The validity of the Boussinesq approximation for liquids and gases, *Int. J. Heat Mass Transfer* **19**, 545–551 (1976).
7. M. A. Langerman and P. D. Bayless, On the validity of the Boussinesq approximation for calculating decay heat removal rates via natural circulation along test reactor plate fuel, *Proceedings of the 1992 ASME Winter Annual Meeting*, ASME HTD-Vol 209, pp. 91–100, Anaheim, California (1992).
8. Z. Y. Zhong, K. T. Yang and J. R. Lloyd, Variable property effects in laminar natural convection in a square enclosure, *J. Heat Transfer* **107**, 133–138 (1985).
9. D. N. Mahony, R. Kumar and J. Bishop, Numerical investigation of variable property effects on laminar natural convection of gases between two horizontal isothermal concentric cylinders, *J. Heat Transfer* **108**, 783–789 (1986).
10. M. Miyamoto, H. Kajino, J. Kurima and T. Takanami, Development of turbulence characteristics in a vertical free convection boundary layer, *Heat Transfer 1982*, Vol. 2, pp. 323–328 (1982).
11. L. Martin, G. D. Raithby and M. M. Yovanovich, On the low Rayleigh number asymptote for natural convection through an isothermal, parallel-plate channel, *J. Heat Transfer* **113**, 899–905 (1991).
12. W. M. Kays and M. E. Crawford, *Convective Heat Transfer* (2nd Edn), pp. 45–57. McGraw-Hill, New York (1980).
13. B. Gebhart, Buoyancy induced fluid motions characteristic of applications in technology—The 1978 Freeman scholar lecture, *J. Fluids Engng* **101**, 5–27 (1979).
14. S. V. Patankar and D. B. Spalding, A calculation procedure for heat, mass, and momentum transfer in three-dimensional parabolic flows, *Int. J. Heat Mass Transfer* **15**, 1787–1806 (1972).
15. A. J. Baker, *Finite Element Computational Fluid Mechanics* (1st Edn), pp. 345–346. McGraw-Hill, New York (1983).
16. M. A. Langerman and E. C. Lemmon, A multi-dimensional finite element MHD model of internal plasma flows, *Proceedings of the 28th National Heat Transfer Conference*, ASME HTD-Vol. 161, pp. 121–130, Minneapolis, Minnesota (1991).